Chapter 1 *Introduction and Literature Review*

1.1 Introduction

1.1.1 Transition Metal Oxides

Nanostructured binary transition metal oxides (TMOs) represent a crucial category of smart materials highly esteemed for their exceptional chemical stability, straightforward structure, and cost-effective production methods. These materials serve as fundamental elements for the advancement of next-generation electronic devices. TMOs hold widespread appeal across industries due to their myriad technological applications, addressing contemporary challenges in cutting-edge research. In TMOs, electrons occupy the s-shells of metal cations, while the d-shells contain partially filled unpaired electrons, resulting in distinctive physical and chemical attributes. Nanostructured TMOs, unlike their bulk counterparts, offer enhanced structural, optical, magnetic, electronic and electrical properties [1–3]. A variety of TMOs, such as TiO_2, VO_2, MnO_2, Fe_2O_3, NiO, ZnO, WO_3, ZrO_2 and HfO_2, featuring diverse morphologies and dimensions, are being investigated for a wide spectrum of industrial applications. Ongoing research and development endeavors have identified promising roles for TMOs in water desalination and purification, transparent semiconductor devices, spintronics, gas sensing, scintillation, UV detection, photocatalysis, optoelectronics, energy storage, memory devices, fuel cells, optical coatings and abrasive materials. Furthermore, non-toxic, lead-free TMOs have garnered attention for biological applications, including antibacterial agents, biosensing, bio transportation, radiosensitization, and drug discovery and delivery [4–8].

When size of the materials is reduced to the nanometer scale, their physical and chemical properties often undergo significant constructive modifications [9,10]. A clear example of this can be seen in Fe_2O_3 nanoparticles, where antiferromagnetic Fe_2O_3 transforms to superparamagnetic behavior when the particles are around 3 nm in size [11–13]. This size reduction, resulting in a high surface-to-volume ratio, imparts unique properties to TMOs. Various TMO nanostructures, such as nanoplates, nanorod arrays, nanotubes, nanobelts, nanoforests and nanobrushes can be synthesized using methods such as sol-gel, hydrothermal, solvothermal, liquid/vapor phase methods and thermal decomposition. The morphology of these nanostructured TMOs can be finely tuned by adjusting synthesis parameters, including temperature, pressure, gas flow, solvents and surfactants [14–21].

Another example of the impact of nanostructuring is observed in TiO_2 nanoparticles. TiO_2 has three crystal structures: anatase, rutile and brookite. Research has shown that reducing the particle size below 14 nm makes the anatase phase more stable than the rutile phase. Above this critical size, the rutile phase can be stably maintained under ambient conditions [22–25]. Thus, nanoscale engineering of TMOs allows enhanced control over their structural, optical, magnetic, electrical and other properties. Hafnium oxide (HfO_2) is particularly noteworthy because of its excellent thermodynamic stability and its potential to address challenges in the silicon-based industry across a wide range of applications [26].

1.1.2 HfO_2 and its Crystal Structure

HfO_2, also known as hafnia, was initially utilized as a refractory ceramic material in reactors and thermocouple devices due to its high melting point, before its potential application as an electronic material in complementary metal oxide semiconductor

(CMOS) technology. HfO_2 shares nearly identical physical and chemical properties with ZrO_2. After the discovery of transformation toughening in crystalline ZrO_2, extensive research has been undertaken to investigate the crystallographic properties of crystalline HfO_2. The crystallography of HfO_2 significantly influences its various physical properties, including structural, electronic, magnetic and optical characteristics. In its bulk form, HfO_2 displays polymorphism with monoclinic (m), *P21/c*, tetragonal (t), *P42/nmc* and cubic (c), $Fm\bar{3}m$ phases. These distinct structures can exist at different temperatures under normal pressure, as depicted in **Figure 1.1**.

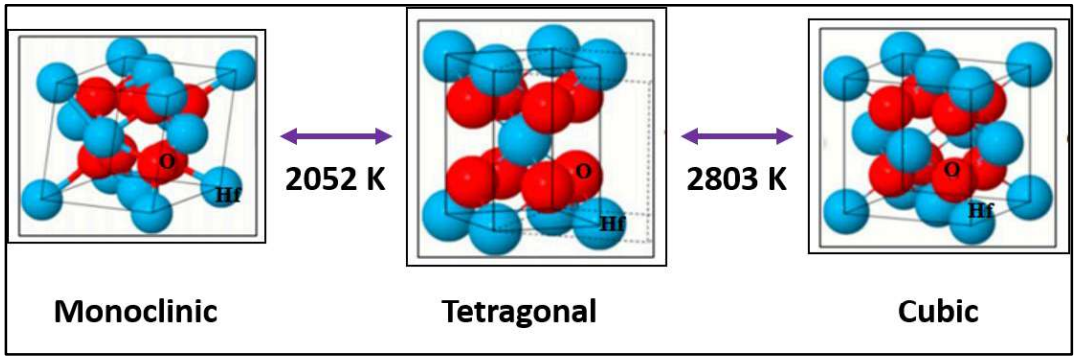

Figure 1.1 *Three crystal phases of HfO_2 as a function of temperature under ambient pressure.*

In contrast to ZrO_2, HfO_2 undergoes phase transformations among its three phases at relatively higher temperatures. Thermodynamic investigations suggest that these transformations, from monoclinic to tetragonal and ultimately to cubic, are influenced by internal energy and entropy [27]. The Gibbs free energy equation ($\Delta G = \Delta U + p\Delta V - T\Delta S$) is crucial for comprehending these phase changes in HfO_2, where ΔG, ΔU, ΔV *and* ΔS denote changes in Gibbs free energy, internal energy, volume and entropy, respectively, with pressure represented by p and the phase transformation temperature by T. The high temperature tetragonal and cubic phases of HfO_2 are more stable owing to their higher

symmetry and entropy. At the phase transition point, ΔG must be zero, indicating minimum energy conditions. First-order phase transitions exhibit discontinuities in the first derivatives of G (entropy and volume), while second-order transitions show continuous first derivatives, indicating no change in S or V.

In bulk HfO_2, the monoclinic phase remains stable at room temperature, transitioning to the tetragonal phase at approximately 2052 K, and then to the cubic phase at 2803 K [28]. Various factors such as particle size, impurities and stress can influence the temperature of these transformations. In the monoclinic phase, Hf^{4+} has a coordination number of 7, which increases to 8 in the higher temperature tetragonal and cubic phases [29,30]. The monoclinic to tetragonal phase change represents a first-order transition due to significant local bonding alterations and a notable reduction in lattice volume, resulting in substantial crystal strain. Conversely, the tetragonal to cubic transition is second-order, as it does not entail significant volume changes [31].

Additionally, under external pressure, the monoclinic phase of HfO_2 becomes unstable. The temperature-pressure (*T-P*) phase diagram shows that HfO_2 adopts orthorhombic symmetry under high pressure, forming two polymorphs known as Ortho I (*OI*) and Ortho II (*OII*), as depicted in **Figure 1.2**. These high-pressure phases are stable between 4 to 25 GPa and remain stable up to 1400 °C [32]. Neutron diffraction studies reveal that *OI* stabilizes in the *Pbca* space group, while *OII* adopts an orthorhombic cotunnite ($PbCl_2$) type structure with the *Pmnb* space group. In the *OI* phase of HfO_2, Hf^{4+} ions are coordinated with oxygen in a 7-fold manner, whereas in the *OII* phase, the coordination increases to 9-fold [33,34]. The transition from the monoclinic phase to the *OI* phase involves a volume reduction. The shift from the *OI* to the *OII* phase occurs at pressures that do not match thermodynamic equilibrium conditions due to the reconstructive nature

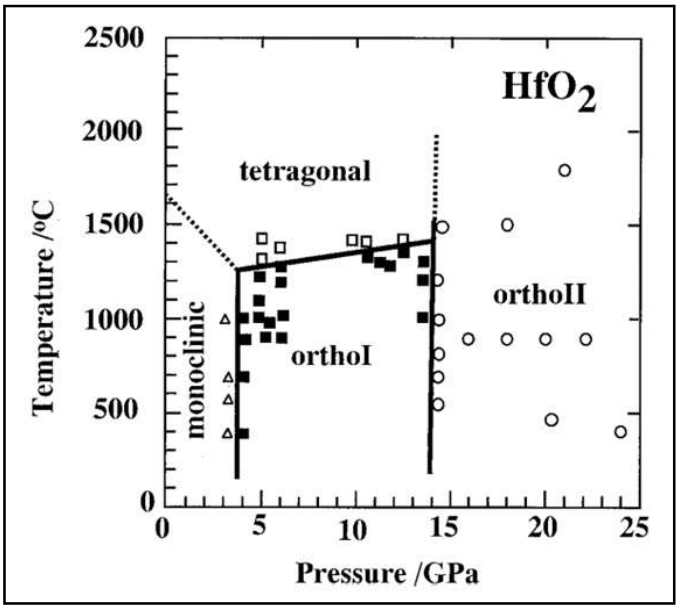

Figure 1.2 *Phase diagram of Temperature vs. Pressure HfO_2* [32].

of the transition. Based on first principle calculations and experimental data, the high-pressure *OII* phase of HfO_2 is considered promising for ultrahard materials because of its excellent bulk modulus property.

1.1.3 Physical and Chemical Properties of HfO_2

HfO_2 is a chemically and thermodynamically stable electrical insulator with a wide bandgap of approximately 5.7 eV and an appropriate dielectric constant (*k*). This makes it an efficient material to overcome major challenges in the current complementary metal oxide semiconductor (CMOS) technology [35,36]. In CMOS devices, scaling down the gate dielectric thickness below 3 nm leads to higher leakage current due to direct electron tunneling. To address this, high-*k* materials like HfO_2 are preferred, as they enable the production of high performance CMOS devices [37]. In 2007, Intel incorporated HfO_2 into its 45 nm technology, replacing conventional SiO_2, which significantly reduced leakage current density by an order of magnitude and mitigated heat dissipation issues in

the 45 nm technology node [38]. Besides its high-*k* value, HfO_2 has other notable physical properties, such as high density of ~ 9.8 g/cm³ and very high melting point of ~ 2750 °C with a refractive index of about 2. The intriguing properties make HfO_2 suitable for various applications, including optical coatings, X-ray phosphors, anti-reflective coatings, refractories and advanced memory devices based on resistive switching and ferroelectricity [39–43]. These applications highlight the multifaceted utility of HfO_2 nanoparticles and thin films in advancing technology and healthcare. An illustrative diagram of various applications of HfO_2 is shown in **Figure 1.3**. In this thesis, we have explored the sensor and resistive switching based memory device applications of HfO_2 nanostructures.

Figure 1.3 *Different applications of HfO_2 nanostructures in various industries.*

1.2 Literature Review

1.2.1 Green Synthesis

Metal oxide nanoparticles are inspiring materials that have unique characteristics and wide range of applications. Among physical, chemical and biological synthesis methods of nanoparticles, the chemical approach, consisting of sol-gel synthesis, coprecipitation method, combustion and hydrothermal techniques, etc., has received the greatest attention in recent years due to ease of production and high yield. As compared to precursor chemicals, the substance produced chemically is either less toxic or similarly harmful [44,45]. The chemically synthesized nanoparticles would still have certain undesirable characteristics such as high cost, long reaction time, high energy equipment, toxic byproducts, etc. This barrier is the main cause of the present growth of environment-friendly green synthesis of nanoparticles. We can get nontoxic byproducts by the development and usage of efficient alternatives, such as synthesizing nanoparticles using plant extracts. The byproducts are more ecologically friendly since the production processes are considerably more similar to those found in nature. As a result, the fundamental ideas of green synthesis, which call for utilizing harmless materials and reducing waste and pollution, are being adopted in various sectors. Plant extracts used to biosynthesize metallic and metal oxide nanoparticles contain a variety of secondary metabolites and bioactive chemicals, such as flavonoids, alkaloids, terpenoids, phenolic compounds and enzymes that aid in reducing metal ions and stabilizing nanoparticles.

Leaf extracts of *C. fistula* and *M. azedarach* undergo physio-chemical alterations in the aqueous solution when zinc acetate dihydrate is added [46]. Here, the most noticeable factor is the color change that may be seen in the reaction mixture within a short period of time. This is regarded as the first indication of nanoparticle formation. The conversion

of Zn ions to ZnO nanoparticles is hypothesized to be caused by flavonoids and phenolic substances. The color of the solution stops changing after a few hours, indicating that the ZnO salt had fully undergone bioreduction to become nanoparticles. The synthesis of the nanoparticles is thought to be greatly influenced by temperature. Furthermore, it is well known that the size of the nanoparticles decreases with increasing reaction temperature during the synthesis. As a result, the reactants are incubated at a considerably higher temperature of 70 °C, which results in the formation of extremely small sized ZnO nanoparticles. Darroudi *et al.* have used Gelatin (type B) for synthesizing ZnO nanoparticles to study the cytotoxicity effects [47]. It is discovered that the production of ZnO nanoparticles in gelatinous medium is equivalent to that of standard reduction techniques utilizing hazardous polymers or surfactants. CuO and ZnO nanoparticles are synthesized by Maruthupandy et al. using *C. japonica* leaf extract for optical sensor applications [48]. Different sizes of ZnO nanoparticles are synthesized by *Parthenium hysterophorus* plant extracts to study the antifungal activity with respect to the particles size [49]. Further, Sharma *et al.* synthesized CuO nanoparticles of 30-40 nm by green synthesis method using *Calotropis gigantean* leaf extract [50]. A few other reports on the green synthesis of metal oxides are listed in **Table 1.1**.

Controlling particle size and shape as well as attaining monodispersity in the solution phase are common challenges for the bio-production of nanoparticles. Normally, nanoparticles are synthesized using complex procedures and the outcomes depend on numerous parameters. If the intended particle size is extremely small, precise control of the parameters is required. Although there are many variables that can impact the green synthesis of metal oxide nanoparticles, there have been several attempts to resolve these issues by adjusting growth parameters such as light, pH, reactant concentration, temperature and incubation period.

Table 1.1 *List of green synthesis of metal oxide nanoparticles with used green source and remarks on the applications of green nanomaterials.*

Author (Year)[Ref]	Synthesized Material	Green Source	Applications
Naiel *et al.* (2022) [51]	ZnO	Limonium Pruinosum	Anti-skin cancer, antimicrobial and antioxidant potentials
Faisal *et al.* (2021) [52]	ZnO	Aqueous Fruit Extracts of Myristica fragrans	Excellent antibacterial antioxidant, biocompatible and photocatalytic nanomaterial
Shah *et al.* (2022) [53]	Fe_3O_4	Peltophorum pterocarpam leaf extract	Better photocatalytic activity
Zare *et al.* (2019) [54]	ZnO-Ag	Thymus vulgaris leaf extract	Better antimicrobial activity against food-borne pathogen, and biocompatibility
Thi *et al.* (2020) [55]	ZnO	Orange fruit peel extract	Strong antibacterial activity towards Escherichia coli
Dehury *et al.* (2023) [56]	ZnO	Orange fruit peel extract	Better selectivity for liquid ammonia sensing

1.2.2 Structural Transformation in HfO_2: Effect of Synthesis Parameters and Dopants

Phase stabilization in transition metal oxides (TMOs) typically involves maintaining a specific crystalline phase at ambient conditions that is usually observed only at high temperatures and pressures. Achieving this stability under normal conditions often requires alloying with appropriate dopants or optimizing synthesis parameters such as temperature, grain size, solvent and oxygen partial pressure. It is important to find a way to stabilize the high-temperature tetragonal or cubic phase of HfO_2 at room or moderate temperatures, as these phases exhibit unique physical properties absent in the monoclinic phase. For CMOS device applications, HfO_2 is used in its amorphous phase at growth

temperatures around 300 °C, which does not possess superior physical properties compared to the crystalline monoclinic phase. First principle calculations indicate that the high temperature tetragonal or cubic phases of HfO_2 are more technologically significant than the monoclinic phase. The monoclinic phase has a low *k* value of about 15, whereas the tetragonal or cubic phases have higher *k* values above 30 [57]. Thus, using HfO_2 in its high-symmetry tetragonal or cubic phases is more advantageous for developing future CMOS devices with improved performance and reliability.

The cubic phase of HfO_2 can be stabilized at room temperature without dopants. This metastable cubic phase can be achieved in HfO_2 films annealed at 500 °C in a vacuum. The transition from the amorphous to the cubic phase occurs between 30 °C and 1500 °C. The cubic phase remains stable up to 600 °C and partially transforms to the monoclinic phase at temperatures up to 1400 °C, with this transformation becoming more pronounced when HfO_2 films are annealed in air. Sharath *et al.* demonstrated that the high-temperature tetragonal phase can be achieved in HfO_2 films deposited on $TiN/SiO_2/Si(001)$ at a substrate temperature of 320 °C, as shown in **Figure 1.4** [58].

While stoichiometric HfO_2 crystallizes in the monoclinic phase, oxygen deficient HfO_2 tends to exhibit the tetragonal phase. The stabilization of high temperature tetragonal or cubic phases in HfO_2 films is mainly influenced by the concentration of oxygen atoms and vacancies, as well as the post-deposition annealing temperature and environmental conditions. These phases can be made more stable by carefully controlling and optimizing the oxygen content in the film. Additionally, factors like grain size and grain boundary energy play critical roles in these phase transformation processes.

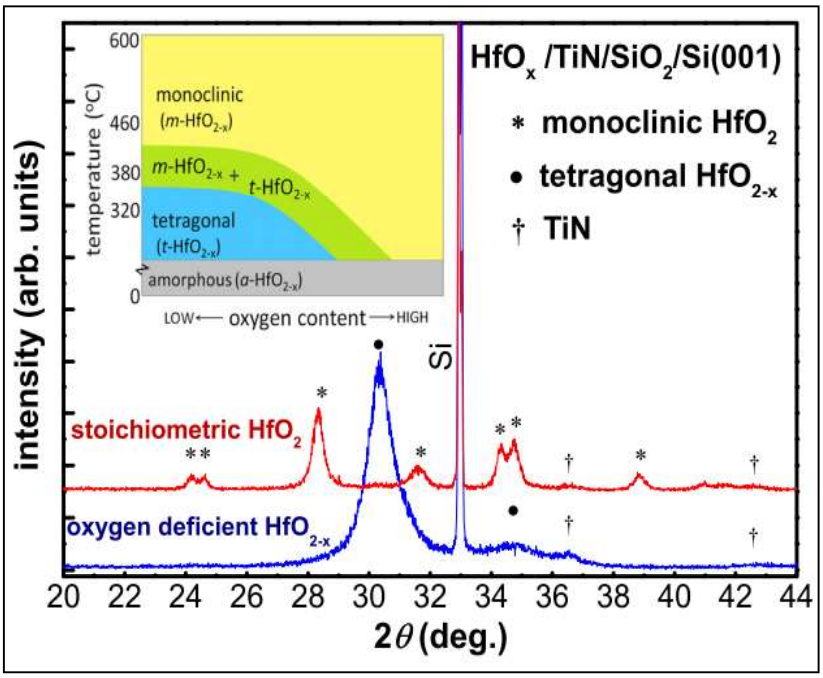

Figure 1.4 *X-ray diffraction patterns indicating stabilization of the monoclinic and tetragonal phase in stoichiometric and oxygen deficient HfO_2 films* [58].

Besides stabilizing the tetragonal or cubic phases at room temperature in HfO_2 films, a similar cubic phase can be achieved in HfO_2 nanoparticles. **Figure 1.5** shows the direct precipitation of the monoclinic and cubic phases of HfO_2 using an appropriate solvent, without the need for surfactants or post-synthesis treatments like heating. The cubic phase of HfO_2 can be obtained with a more reductive solvent. By optimizing synthesis parameters, effective preparation techniques have been developed to produce high-quality cubic HfO_2 nanoparticles that remain stable under ambient conditions [59]. Thus, by fine-tuning the stoichiometry of nanostructured HfO_2, it is possible to maintain the high-temperature cubic or tetragonal phase at room temperature without any dopants. However, this stabilized cubic or tetragonal phase is prone to transforming into the less desirable monoclinic phase with even slight temperature changes.

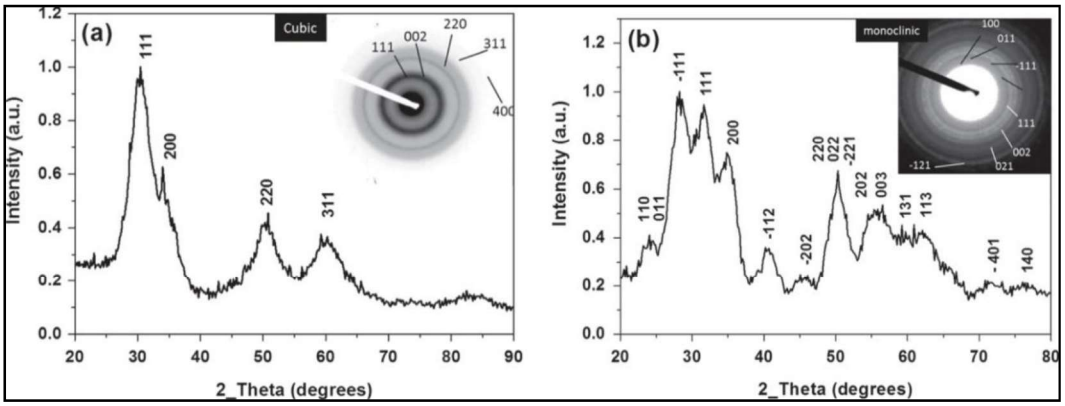

Figure 1.5 *X-ray diffraction data of (a) cubic and (b) monoclinic HfO_2 nanoparticles. Selected area electron diffraction (SAED) patterns of respective phases are displayed in the insets* [59]**.**

Doping of Trivalent Ion

Introducing trivalent ions as dopants is a notable approach to controlling the phases of HfO_2 and stabilizing them under normal conditions. The concept revolves around the insertion of trivalent ions into the HfO_2 lattice, which proves effective in altering the oxidation states, particularly due to the difference between the dopant and Hf cation. When a trivalent ion replaces Hf^{4+} in the lattice, it generates an electron, disrupting the charge balance and leading to the creation of oxygen vacancies to compensate for these electrons [60]. The stabilization mechanism of tetragonal or cubic HfO_2 largely hinges on the variance between the ionic radii of the dopant and Hf cations. If the trivalent ion has a smaller ionic radius than that of Hf, it stabilizes the tetragonal phase by reducing the relative energy with respect to the monoclinic phase significantly. This causes the nearest oxygen atoms to shift towards the dopant sites, displacing other oxygen atoms outward due to structural relaxation. Conversely, replacing Hf atoms with larger dopants elongates the bond length between the dopant and oxygen atoms, resulting in lower lattice strain compared to tetragonal HfO_2, thereby stabilizing the cubic phase at room temperature [61].

In the monoclinic phase of HfO_2, oxygen atoms can have two different configurations: they can be coordinated with Hf in either a three-fold or four-fold manner. Conversely, in the tetragonal or cubic phases, all oxygen atoms have identical local environments. Oxygen vacancies in tetragonal or cubic HfO_2 tend to occupy the four-fold coordinated Hf sites, reducing the Hf coordination number to 7 and decreasing the concentration of nearby oxygen atoms. This rearrangement causes oxygen atoms to move closer to dopants rather than Hf atoms, forming eight-fold coordination with the dopant and resulting in more 7-fold coordinated Hf atoms in the lattice. First principle calculations indicate that the stability of tetragonal and cubic phases of HfO_2 can be achieved by incorporating undersized dopants like Al and P, as well as oversized dopants such as Y, Gd and Sc [61]. These dopants cause compressive/expansive strain that favors the higher symmetry phases which can accommodate such strain. Experimental evidence has shown that the cubic phase can be stabilized at room temperature using trivalent rare earth (RE) ions like Lu and Eu, which have larger ionic radii than Hf [62]. However, these studies do not thoroughly discuss the stabilization of the high-temperature phase of HfO_2.

Doping of Tetravalent Ion

Considering the ionic radius of tetravalent ions, a similar stabilization of the tetragonal and cubic phases is observed in nanostructured HfO_2. This has been experimentally demonstrated in Ce doped HfO_2, where the larger ionic radius of Ce compared to Hf stabilizes the cubic phase of HfO_2 at room temperature [63]. However, the stability of the tetragonal phase in HfO_2 with smaller tetravalent dopants is less certain. Recently, doping with undersized tetravalent Si has revealed an unusual orthorhombic (*O*) phase in HfO_2 films, distinct from the centrosymmetric orthorhombic phase seen under high-pressure conditions. The polar *O* phase in HfO_2 films shows potential for ferroelectric

properties [64]. Similar behavior has been noted in ZrO_2 doped with Mg [65]. The non-centrosymmetric orthorhombic phase in HfO_2 films has been extensively studied with various dopants, including Mg, Ba, Sr, Y, La, Nd, Sm, Er, Al, Ga, In, Co, Ni, Ge and Zr [66].

The stabilization of the polar orthorhombic phase in HfO_2 by Zr doping is particularly noteworthy for its excellent ferroelectric properties and lower crystallization temperatures compared to Si-doped HfO_2 films. Zr-doped HfO_2 also offers a broader composition range. Various deposition techniques, such as atomic layer deposition (ALD), sputtering, and pulse laser deposition, can achieve this orthorhombic phase in doped HfO_2. The emergence of a non-polar orthorhombic phase in bulk HfO_2 under pressure provides a different explanation for the polar orthorhombic phase in nanostructured HfO_2. According to first principle calculations, significant surface energy effects due to reduced grain size could stabilize this orthorhombic phase [67]. However, these calculations consider a specific grain size, while polycrystalline oxides have a distribution of grain sizes. Understanding the polar *O* phase in Zr doped HfO_2 also involves factors like film thickness, asymmetric stress, top capping electrode, dopant and annealing temperature [68]. Additionally, the polar *O* phase can be achieved in film thicknesses of approximately 10 nm or less on Si substrates, making it suitable for practical applications like non-volatile memory, specifically FeRAM. Systematic retention tests of HfO_2 based FeRAM show promising features due to appropriate relative permittivity and coercive field compared to standard perovskite based ferroelectrics.

1.2.3 HfO_2 Nanostructures for Sensor Application

Sensors allow us to detect various forms of critical information from our surroundings and convert this data into usable formats through specific mechanisms, fulfilling diverse

needs in industries, environmental monitoring and healthcare. Among all, the most commonly used sensors are gas and liquid sensors. These sensors primarily aim to identify chemicals that pose health risks to humans or exist in concentrations below the human olfactory threshold (ppm/ppb levels) [69–71]. In environmental assessments, gas sensors monitor the concentrations of toxic gases and volatile organic compounds to ensure the environment is safe for human habitation [72,73]. In industrial settings, gas sensors help regulate the levels of combustible and explosive gases. Its use has become more widespread with the increasing reliance on natural gas and hydrogen. Breath analysis is another significant application of gas sensors. Ethanol sensors, for example, are used in road safety to quickly determine if a driver is under the influence of alcohol and to quantify ethanol intake [74,75]. In the medical field, non-invasive breath analysis using gas sensors can improve diagnostics; for instance, measuring acetone levels in breath can indicate diabetes [76]. Furthermore, gas sensors are crucial for detecting automotive exhaust gases, monitoring conditions in aquaculture and many other applications [77,78]. Moreover, liquid sensors play a vital role for the detection of toxic compounds in the laboratory and industrial wastes. Liquid sensors are also crucial for detecting toxic compounds in the water supply systems of homes, commercial establishments, industry and irrigation. It is extremely desirable to develop sensors that have excellent selectivity, sensitivity, reversibility and durability combined with microelectronic circuitry and software. An adequate set of metrics, such as sensitivity selectivity, response/recovery time, operating temperature, life cycle, etc., are used to assess the performance of a sensor. Like other metal oxides, HfO_2 is a potential material for different sensing applications. However, only a few reports are available on HfO_2 based sensors. HfO_2 nanostructure based sensors are used for the detection of humidity

and propane along with the detection of toxic gases (CO, NO_2). Also, HfO_2 is used as the pH and refractive index sensor, as reported earlier [79] [80,81].

Ammonia (NH_3) is a highly toxic, colorless, irritant gas with a typical pungent, suffocating odor that is harmful to the environment [82], [83]. When breathed in for an extended period of time, it might induce fatal respiratory disorders. As per the USA "Occupational Safety and Health Administration" (OSHA), NH_3 has a currently allowed "time weighted average" (TWA) exposure limit of 50 "parts per million" (50 ppm) in any "8-hour work shift of 40-hour work per week" [83]. According to the USA's "National Institute for Occupational Safety and Health" (NIOSH), the modified "immediately dangerous to life or health" (IDLH) concentration for ammonia is 300 ppm [84]. The leakage of NH_3 can have serious consequences on the exposed areas because of its low density and corrosive behavior. Hence, the detection of NH_3 at trace levels in different human operational environments is critical. There is well-explained literature on metal-oxide based NH_3 gas sensors that work on the chemoresistance principle. In such sensors, the surface layer of the oxide adsorbs the reducing gas molecule, thus changing the resistivity of the metal-oxide structure by inserting electrons into the conduction band, which enables electrons to flow [85]. Various factors, such as humidity, temperature, pressure, dust, sensor aging, etc., affect the performance of NH_3 sensors. Liu *et al.* propose a high precision method to compensate for the influence of temperature and humidity on polyaniline-cerium dioxide (PANI/CeO_2) NH_3 sensor [86]. Composites of PANI and niobium carbide MXene (Nb_2CT_x) are used for the detection of NH_3 under a humid atmosphere (~ 87 % relative humidity) and at room temperature [87,88]. Recently, green synthesized ZnO based sensors for ethanol and ammonia gases have been reported [89,90]. However, only a few reports are available for sensing liquid NH_3 using ZnO and Fe_2O_3 nanoparticles [56,91].

1.2.4 HfO_2 Nanostructures for Memory Device Application

Nowadays, resistive random access memory (RRAM), having two terminals based on the resistive switching (RS) behavior, is gaining popularity in the semiconductor industry as it is considered as the future generation nonvolatile memory (NVM) because of its simple metal/semiconductor(insulator)/metal architecture, fast switching speed, scalability, high density integration and low power consumption [92–94]. Since the initial experimental findings in 1967 regarding resistive switching in the Al/SiO_x/Au layered structure, numerous metal oxide insulators have been extensively investigated for their potential application in RRAM devices. Compared to other emerging non-volatile memory technologies like magneto resistive random access memory (MRAM), phase change random access memory (PCRAM) and ferroelectric random access memory (FeRAM), RRAM is easier to integrate due to its simple structure and excellent compatibility with existing processing techniques and scalability [95]. RRAM essentially consists of a metal oxide insulator layer positioned between top and bottom metal electrodes. These non-volatile memory devices store and retrieve information (binary states of 0 and 1) by quickly switching between low and high resistance states (LRS/ON and HRS/OFF) when a bias voltage is applied. Initiating resistive switching typically requires an initial specific bias voltage called the forming voltage (V_F), marking the onset of soft dielectric breakdown. In RRAM, the voltage at which the current sharply increases from HRS to LRS is known as the SET voltage (V_{SET}). The voltage needed to switch from LRS to HRS, called the RESET voltage (V_{RESET}), can occur in either the positive or negative bias region. RRAM can exhibit two types of resistive switching modes: unipolar and bipolar. In unipolar switching, both V_{SET} and V_{RESET} occur regardless of the electrical polarity, in either positive or negative bias regions. In contrast, in bipolar mode, V_{SET} and V_{RESET} appear in opposite bias regions. Unipolar operation in RRAM requires a higher current

for the reset process compared to the bipolar mode because thermal effects dominate the reset process in unipolar mode [95]. **Figure 1.6** shows a typical current-voltage (*I-V*) diagram of the resistive switching process [96].

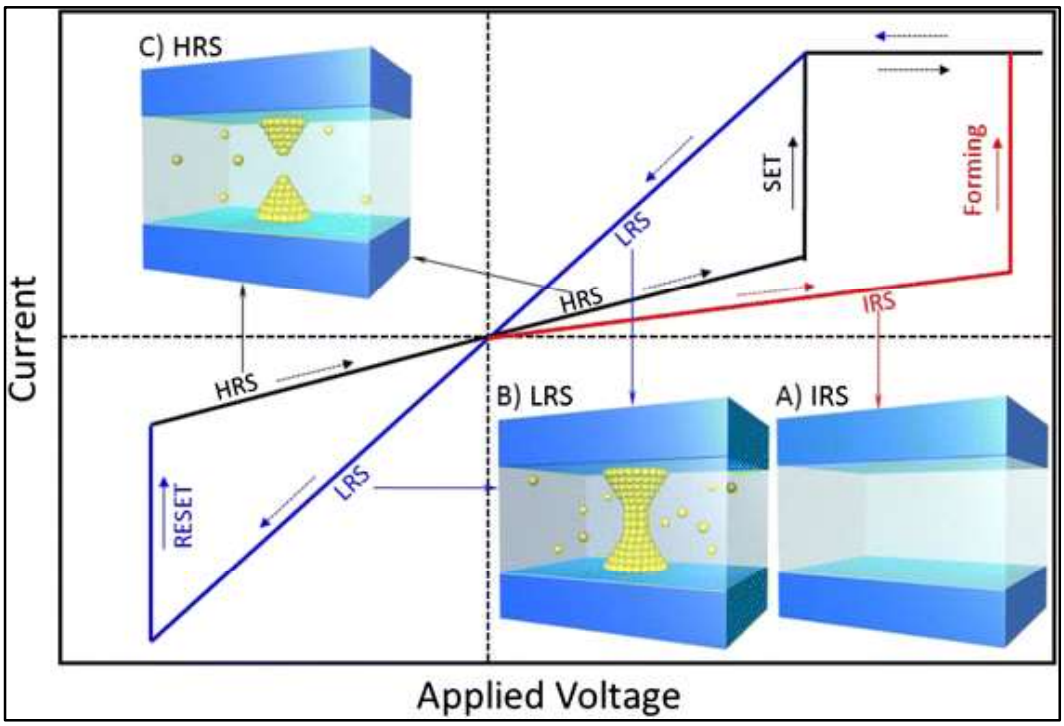

Figure 1.6 *A typical current-voltage (I-V) diagram depicting different processes of resistive switching* [96].

The resistive switching effect is more likely to be observed due to the electrochemical oxidation (metal ion diffusion into the active layer) and migration of oxygen vacancies (V_os) existing in the active layer [97]. Ensuring firm control of the consistency among the devices and operating at low energy are, in fact, the key challenges for developing high performance RRAM devices. It has been demonstrated that the creation of several nanosized conductive filaments (CFs) comprised of charged V_os or transportable metallic ions gives rise to resistive switching characteristics [95]. The formation and rupture of

these CFs, which occur within the active layer, are used to describe the switching between HRS and LRS. To achieve resistive switching behavior, a voltage known as the forming voltage is needed initially in most devices. In this context, the conduction properties of the RRAM device are found to be heavily affected by the deposition of active layer material. As a matter of fact, the active layer can tune several characteristic parameters, including the resistance ratio between HRS and LRS, the forming voltage, and the SET/RESET voltages. Several transition metal oxides, for example, ZnO, TiO_2 and HfO_2, are immensely investigated for the active layer in RRAM devices [98–100]. ZnO based RRAM devices with high durability and stability, low power consumption and self-current compliance have been investigated by Tian *et al.* along with the cytotoxicity test for biocompatibility of the devices [101]. Controlled bipolar resistive switching behavior of TiO_2 and nickel oxide (NiO) thin film based RRAM devices have been explored along with the mimicking of the synaptic behavior [97,102]. Among the transition metal oxides, HfO_2 has emerged as a prospective candidate for the active layer in RRAM applications in forthcoming memory devices owing to its superior performance and better thermodynamical stability over silicon. In this regard, it has been reported that an RRAM device based on HfO_2 exhibits stable, uniform and repeatable bipolar resistive switching [103,104]. Kumar *et al.* report stable, forming free, bipolar RRAM devices based on RE (Dy/Sm) doped HfO_2 thin films [105]. By changing various fabrication parameters, such as deposition/annealing temperature, oxygen partial pressure, thickness of the film, material of top/bottom electrode and selecting the right dopant, it is possible to significantly tune the resistive switching behavior in HfO_2. For instance, in oxygen deficient HfO_2 films displaying substantial reduction of the forming voltage, Sharath *et al.* study the thickness independent switching behavior [58]. By changing the material (TiN/Ti, Cu, Pt, Ni and Ta) for the top metal electrode, Lin *et al.* describe the nonpolar

and bipolar resistive switching performance of HfO_2 based RRAMs. Due to metal cation migration, localized Joule heating effect and electrochemical metallization, the nonpolar resistive switching is detected with only Cu and Ni electrodes [106]. Chen *et al.* used a voltage-biased scanning probe microscope (SPM) tip as a microelectrode to control the directional transport of oxygen anions in the HfO_x nanofilm to form a single conductive filament, resulting in a significant improvement in the reliability and stability of the RRAM device performances [107]. Regulated resistive switching behavior is reported in Al doped HfO_2 based RRAM, perceived due to induction and controlled evolution of CFs [108]. By varying the concentration of oxygen vacancies, Akbari *et al.* demonstrate the forming-free performance of Ni doped HfO_2 RRAM devices in their investigation of Ni and Ta doped HfO_2 based memory devices [109]. Thin film based RRAM devices are reported by varying the film thickness and adding metal (Ag and Cu) layers to enhance the resistive switching performance [110,111]. Thickness dependent nickel ferrite films have been used for resistive switching where the highest storage window is observed at an optimum thickness due to the critical grain microstructure with suitable film thickness, which could preferentially gather oxygen vacancies along the grain boundaries to assist the formation of CFs easily [110]. The strategies of filament control for improving resistive switching performance are also evaluated from the aspects of electrode optimization, switching layer optimization and channel design [112]. **Table 1.2** lists a brief literature survey on controlling the conductive filaments using the above three methods.

The predominant current conduction mechanisms during both the SET and RESET processes in RRAM involve several models, such as Schottky emission, Ohmic conduction, Poole-Frenkel emission, Fowler-Nordheim tunneling and space charge limited current. These mechanisms function in both the low resistance state (LRS) and

Table 1.2 *A brief list of reports for optimizing resistive switching performance using filament control.*

Author (Year)[Ref.]	**Filament control strategy**	**Device structure**	**Used Technique**	**Optimized Performance**
Shin *et al.* (2016) [113]	Electrode optimization	$Ag/Al_2O_3/Pt$	Ag pyramid electrode	Reduced and stabilized V_{SET} and V_{RESET}
Chen *et al.* (2019) [114]	Electrode Optimization	$Pt/HfO_2/Pt$	Voltage biased scanning probe microscope tip microelectrode	Improved retention and stability of switching voltage
Liu *et al.* (2016) [115]	Switching layer optimization	Ag/ZrO_2/graphene/Pt	PMMA assisted graphene transfer	Increased retention and endurance
Zhao *et al.* (2017) [116]	Switching layer optimization	Cu/graphene/HfO_2/Pt	Electron beam lithography and oxygen plasma etching	Increased retention and endurance
Huang *et al.* (2014) [117]	Switching layer optimization	ITO/ZnO:Ga/ZnO/ITO	Solution growth of Ga	Uniform distribution of resistance state
Choi *et al.* (2018) [118]	Channel Design	$Ag/Si_{0.9}Ge_{0.1}/Si$	Construction of 1D channel by defect selective etch	Improved endurance and stability of V_{SET}

high resistance state (HRS). In the LRS, current-voltage behavior is typically linear and follows the Ohmic model. In contrast, the HRS exhibits non-linear current-voltage characteristics, including Schottky emission (where $\log(I)$ is proportional to $\sqrt{V}$), Poole-Frenkel (P-F) emission (where $\log(I/V)$ is proportional to $\sqrt{V}$), Fowler-Nordheim (F-N) tunneling (where I/V^2 is proportional to V^{-1}) and space charge limited current (SCLC)

(where I is proportional to V^2) [95,119]. The resistive switching in RRAMs is explained through various mechanisms such as the formation of CFs, migration of oxygen vacancies or ions, modulation of the Schottky barrier, cation migration and the trapping of charged carriers present either at interfaces or dispersed within the metal oxide insulator film [120].

As the field of artificial intelligence (AI) and machine learning (ML) increasingly rely on complex algorithms, the conventional von Neumann computing architecture faces periodic challenges to its credibility [121]. Simply adhering to traditional von Neumann architecture or relying on Moore's law, which has dominated the electronic industry for the past five decades, cannot effectively bridge the performance gap in computing. To meet the demands of future computing, new device concepts, materials and architectures are being explored. In recent years, there has been a significant increase in research focused on neuromorphic computing architectures inspired by the human brain, addressing key AI/ML needs such as cognitive tasks, fault tolerance, high processing speed, precision and low power consumption [122,123]. In the brain, synapses (junctions between neurons) are vital for memory, processing and learning. Artificial synapses created using two-terminal memristors can effectively mimic the complex ion dynamics, such as Ca^+ and Na^+, seen in biological synapses involved in synaptic plasticity [124,125]. These memristors, with their ability to exhibit both short-term and long-term retention loss, can replicate various synaptic functions like pair pulse facilitation (PPF), potentiation, depression, spike time-dependent plasticity (STDP) and Pavlovian associative learning. These capabilities are directly applicable to tasks such as image processing, sparse coding and data classification. Additionally, the random switching behavior of memristors can be utilized as random number generators for data encryption and cybersecurity [121]. Most existing memristors, which rely on drift

mechanisms and exhibit nonvolatile switching (NVS) behavior, have difficulty in accurately mimicking short-term synaptic plasticity. However, a new class of diffusive memristors, based on the migration of Ag or Cu ions, has been recently developed [124–126]. These memristors display volatile switching (VS) behavior with short-term memory (STM) loss, similar to the Ca^{+} and Na^{+} dynamics in biological systems. These diffusive memristors can simulate short-term synaptic plasticity, leaky-integrate-fire neurons and nociceptive behavior [127,128]. Utilizing these HfO_2 based volatile memristors enables the development of low-power, scalable and intelligent neuromorphic devices.

1.3 Objectives

HfO_2 has been extensively researched for a leading technological material in past decades due to its high dielectric permittivity (*k*) and excellent thermodynamic stability, along with the other advantages of metal oxides. In contrast to SiO_2, HfO_2 is popularly used for next-generation high-*k* gate dielectrics in microelectronics. HfO_2 possessing the monoclinic phase shows a *k* value of ~ 15, which is four times higher than that of SiO_2 (~ 3.9). The high temperature tetragonal and cubic phases of HfO_2 are technologically more important since they exhibit relatively higher *k* values, such as ~ 70 and 30, respectively. The high-*k* cubic and tetragonal phases can be stabilized at room temperature by doping elements of lower valency than Hf^{4+}. Additionally, the rare orthorhombic phase of HfO_2 can be stabilized in thin films by suitably modulating the deposition parameters, annealing temperature and average grain size. Moreover, considering environmental sustainability and the impact of the conventional synthesis methods of nanoparticles, increased emphases are being directed for adopting environment-friendly green methods. In this context, the stabilization and optimization

of cubic, tetragonal and orthorhombic phases of HfO_2, along with the green synthesis method, is extremely important for its diverse applications. In this work, our goal is to provide a comprehensive exploration of nanostructured HfO_2, focusing on both its structural characteristics and multifunctional attributes. The study is motivated by the potential applications of HfO_2 in optoelectronic devices, advanced sensing technologies and resistive switching devices. The primary objectives of this thesis work include the investigation of the morphological intricacies of HfO_2 nanoparticles and thin films, study of their crystalline structure and evaluation of their multifunctional properties, predominantly in the realms of sensing applications and resistive switching performance.

In this chapter, a concise overview of the physical, structural and microstructural properties of HfO_2 nanoparticles and thin films, along with a brief literature survey on synthesis methods are presented. Our investigation extends to various applications of HfO_2 nanoparticles and thin films, such as physical/chemical sensors and advance memory devices. Here, we have discussed the noteworthy outcomes of the research, summarizing the key contributions in this field. In this thesis, a comprehensive and systematic study on the structure, microstructure, optical, electrochemical and electrical properties of HfO_2 nanostructures is provided. The experimental methodologies, results, discussions and important findings are presented as the following chapters:

Chapter 2 presents a summary of the methodologies utilized for the synthesis of HfO_2 nanoparticles and fabrication of HfO_2 thin films. The chapter also addresses characterization techniques that are used for data collection and calibration.

Chapter 3 discusses the stabilization of the high temperature cubic phase of HfO_2 at room temperature by doping praseodymium (Pr) up to 15 at%. With doping, the average particle size is reduced from 35 to 10 nm, accompanied by enhanced strain estimated

from Williamson-Hall plots. The optical bandgap decreases from 5.42 eV in pure HfO_2 to 5.06 eV in 15 at% Pr doped HfO_2 due to formation of sub-bands by oxygen vacancies near the conduction band. Hence, high temperature cubic phase is stabilized at room temperature due to enhanced oxygen vacancies inducing 8-fold oxygen coordinated Pr^{3+} ions in the lattice.

In Chapter 4, we have studied the sensing properties of green synthesized HfO_2 nanoparticles using orange peel extracts. HfO_2 nanoparticles synthesized with 4 wt% orange peel extract and calcined at 900 ^{0}C for 1 h (HO-4-OPE) show well dispersed particles of size 34 nm with maximum yield. A sensing framework to detect liquid NH_3 is developed using HfO_2 nanoparticle coated electrode and electrochemical impedance spectroscopy. We have successfully detected 50 to 500 ppm of liquid NH_3 concentration with charge transfer resistance as the sensing parameter.

In Chapter 5, we demonstrate the performance of RRAM device using HfO_2 thin films deposited using the ion beam sputtering technique on highly doped Si substrate by varying thickness from 10 to 30 nm with density in the range of 9.1-8.6 g/cm^3. A drastic change in the average grain size from ~ 90 to ~ 2000 nm is noticed, along with a structural transformation from orthorhombic to dominant monoclinic phase when the thickness is increased from 20 to 30 nm. Among all films, the film of 20 nm thickness shows better switching behavior with an ON/OFF ratio of ~ 7, which has been attributed to the appropriate grain size, enhanced crystallization and oxygen vacancies. The endurance and retention characteristics, along with the switching mechanism, are discussed in this chapter.

Chapter 6 describes resistive switching behavior in case of molecular beam epitaxy grown HfO_2 thin films fabricated on p^{++}-Si (100) substrate at substrate temperature of

300 and 500 °C. Both films demonstrate forming free volatile resistive switching behavior with SET voltage of -3.1 and -3.6 V, along with the ON/OFF ratio of ~ 2 and ~ 4 for the films with substrate temperature of 300 and 500 °C, respectively. Memory device based on HfO_2 film with higher substrate temperature exhibits a better ON/OFF ratio due to higher crystallinity and availability of more oxygen vacancies. A comprehensive mechanism of volatile resistive switching is also discussed in this chapter.

In Chapter 7, we have summarized the important findings of this thesis work, along with a discussion of the future prospects.